Micellar Aggregates of Amylose-Block-Polystyrene Rod-Coil Block Copolymers in Water and THF

ARTICLE *in* MACROMOLECULES · FEBRUARY 2005

Impact Factor: 5.8 · DOI: 10.1021/ma0345549 · Source: OAI

Micellar Aggregates of Amylose-*block*-polystyrene Rod−Coil Block Copolymers in Water and THF

Katja Loos,[†,⊥] Alexander Böker,[‡] Heiko Zettl,[‡] Mingfu Zhang,[†,#] Georg Krausch,[‡,§] and Axel H. E. Müller*[,†,§]

Makromolekulare Chemie II, Physikalische Chemie II, and Bayreuther Zentrum für Kolloide und Grenzflächen (BZKG), Universität Bayreuth, 95440 Bayreuth, Germany

Received April 29, 2003; Revised Manuscript Received November 9, 2004

ABSTRACT: Amylose-*block*-polystyrenes with various block copolymer compositions were investigated in water and in THF solution. Fluorescence correlation spectroscopy, dynamic light scattering (DLS), and asymmetric flow field-flow fractionation with multiangle light scattering detection indicate the presence of unimers, oligomers, and large micellar species in THF. Up to four different species were detectable by DLS with hydrodynamic radii ranging from a few nanometers to >10 μm, indicating that the system is not in a thermodynamic equilibrium state. Collapsed aggregates were monitored on a silicon surface by scanning force microscopy and transmission electron microscopy. In water, crew-cut micelles were obtained from the same block copolymers by a single solvent approach, using elevated temperature and pressure. These crew-cut aggregates are much more uniform than the respective star aggregates in THF, and their radii scale with $R_h \propto N_{core}^{1/4}$, $R_h \propto N_{corona}^{1/6}$ in solution and with $R \propto N_{core}^{1/4}$, $R \propto N_{corona}^{1/2}$ on a silicon surface.

Introduction

Spontaneous self-assembly of synthetic molecules and macromolecules offers a means to construct a variety of ordered nanostructures. Such nanoobjects of well-defined shape and size have potential fundamental and practical implications in areas such as materials science, molecular electronics, and biomimetic chemistry. A typical example for macromolecular self-assembly are block copolymers, where different linear homopolymers are linked by covalent bonds. The case of diblock copolymers has been particularly well studied.[1] A variety of different mesostructures are formed in bulk (lamellae, cylinders, gyroids, spheres) if the two homopolymers are sufficiently incompatible. If both blocks are amorphous polymers, the particular morphology formed depends on the total degree of polymerization, N, the Flory−Huggins interaction parameter, χ_{AB} (quantifying the incompatibility between the blocks), and the volume fractions of the blocks.[2]

A possibility for the design of new architectures is the use of blocks of different molecular morphologies, rod−coil diblock copolymers[3] being a prominent example. Various types of rod−coil diblock copolymers have been reported, including block copolymers with a helical segment, e.g., polypeptides,[4] polyisocyanides,[5] polyisocyanates,[6] or polycarbodiimides,[7] block copolymers with a nonhelical rod segment, e.g., aromatic polyamides,[8] polythiophenes,[9] or poly(phenylquinoline),[10] and well-defined rod−coil oligomers.[11] The stiffness asymmetry in rod−coil diblock copolymers results in an increase in χ_{AB} in comparison with coil−coil diblock copolymers. This leads to the formation of self-assembled, phase-separated structures at relatively small degrees of polymerization in comparison to coil−coil block copolymers.[12]

When diblock copolymers are dissolved in a selective solvent, spontaneous self-assembly into aggregates occurs. Different morphologies will form upon variation of the concentration, the quality of the solvent, or the relative length of the two blocks. These morphologies include micelles with spherical, elliptical, or cylindrical cores.[13] Highly asymmetric amphiphilic block copolymers usually form core−shell aggregates, the core being much smaller than the corona. These aggregates are usually referred to as star micelles. In the reverse case the aggregates are referred to as crew-cut micelles.[14] These crew-cut assemblies are usually achieved by dissolving the block copolymer in a common solvent for both blocks and subsequent addition of a selective solvent for the shorter block, which then induces the aggregation of the longer block.[15] A different approach profits from the reduced polymer/solvent interaction parameter at elevated temperature and pressure,[16] which favors the development of crew-cut aggregates.[17]

In the present work we report on amylose-*block*-polystyrene block copolymers (Scheme 1), which were synthesized by a combination of living anionic and enzymatic polymerization.[18] In addition to the increase in χ by means of the conformational asymmetry between the two blocks, this system can form intermolecular hydrogen bonds between neighboring rod segments. Moreover, the helical secondary structure of amylose adds thermotropic and lyotropic liquid-crystalline properties.

Experimental Part

Materials. The synthesis as well as the characterization of amylose-*block*-polystyrene (sequential anionic and enzymatic polymerization) has been reported elsewhere.[18] A summary of all synthesized block copolymers can be found in the Supporting Information (Table S-1). Star micelles were ob-

[†] Makromolekulare Chemie II.
[‡] Physikalische Chemie II.
[§] Bayreuther Zentrum für Kolloide und Grenzflächen.
[⊥] New address: University of Groningen, Polymer Chemistry, Faculty of Mathematics and Natural Sciences, 9747 AG Groningen, The Netherlands.
[#] Present address: University of Massachusetts, Polymer Science & Engineering, Amherst, MA 01003.
* Corresponding author.

10.1021/ma0345549 CCC: $30.25
Published on Web 01/04/2005

Scheme 1. Structure of Amylose-*block*-polystyrene

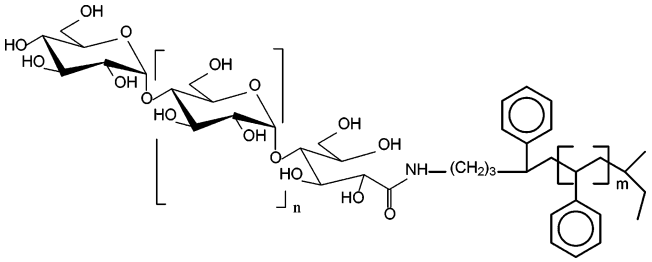

Table 1. Summary of Radii Found in Aqueous Solution (1 g/L) via Dynamic Light Scattering and Scanning Force Microscopy of Block Copolymers with Different Block Copolymer Compositions

N_{PS}	$N_{amylose}$	$R_{h,DLS}$ (z-fraction, %)		$\langle R\rangle_{n,SFM}$	σ
30	60	1.37 (87)	38 (13)	8.5	6
50	60	1.6 (5)	38 (95)	10	3
100	65	2.8 (6)	44 (94)	11.5	3.5
200	60	3.4 (1)	53.2 (99)	12.5	4
300	70	3.9 (1)	56.4 (99)	15.5	11
740	7		18	5.5	1
740	25	4.8 (2)	58 (98)	6.5	2
740	60[a]	7.7 (5)	63 (95)	8	4
740	100	8.4 (8)	71 (92)	12	10
740	150	3.4 (4)	78 (96)	14	6
740	200	8.5 (3)	80 (97)	18.5	5
740	300	9.1 (2)	85 (98)	21.5	3
740	400	9.5 (2)	87 (98)	24.5	9.5

[a] For this composition $\langle R\rangle_n = 4 \pm 1.5$ nm was determined by TEM (Figure 6B).

tained by simply dissolving the block copolymers in tetrahydrofuran (THF, p.A. quality). Crew-cut aggregates were obtained in water (Millipore quality) at high temperature and high pressure (200 °C at 15 bar for 12 h) in a pressure-persistent Schlenk tube.

Analysis. *Fluorescence correlation spectroscopy* (FCS) was conducted on a ConfoCor 2 (Carl Zeiss, Jena) with a 40× C-Apochromat water immersion objective (NA = 1.2) in THF. Rhodamin B was used as the fluorescent dye, which is hardly soluble in THF. The dye concentration was kept at 10^{-8} mol/L for all samples. The diffusion coefficients and the hydrodynamic radii of the dye-carrying particles were calculated on the basis of the waist radius of the laser beam. The waist radius was determined using Rhodamin 6G in water. For fluorescence excitation an Ar^+ ion laser was used (514 nm). The fluorescent light was collected by the same objective and separated from the excitation light by an dichroic mirror and detected by an avalanche photodiode. The fluorescent signal was autocorrelated and the result fitted by a one- and two-particle fits which take triplet excitation into account.

Dynamic light scattering (DLS) measurements shown in Table S-2 (Supporting Information) were performed on a Brookhaven DLS system (BI-200SM) equipped with an He−Ne laser (SP127-35) and a BI-900AT correlation system. Measurements shown in Table 1 and in Table S-3 (Supporting Information) were performed on an ALV goniometer system SP-125 equipped with a He−Ne laser, an avalanche photodiode, and an ALV correlator using the ALV 5000 software.

Asymmetric-Flow Field-Flow Fractionation (AF-FFF) was accomplished in THF using a Postnova Analytics HRFFF-10000 system equipped with an RI detector (RI dn/1000, Postnova), a UV detector (S 3210 UV/vis detector, Postnova), and a multiangle light scattering detector (MALS, Wyatt Technology DAWN EOS, λ = 632.8 nm). (Dimension of the channel = 0.35 mm; cutoff molecular weight of the membrane = 5000; injection volume = 100 μL; cross-flow gradient = 79.5%−0%, parabolic within 16 min; laminar flow out = 1 mL/min.) The refractive index increment of the sample, dn/dc = 0.148 mL/g, was measured with the NFT ScanRef interferometer (λ = 632.8 nm).

Scanning force microscopy (SFM) was performed on a Digital Instruments Dimension 3100 microscope (Nanoscope III, Software 4.42r8) operated in the Tapping Mode (free amplitude of cantilever ≈ 20 nm, amplitude set point ≈ 1.7). The silicon nitride cantilevers were driven some 3% below their resonance frequency (250−350 kHz). The height profiles were measured with a scan velocity of 6 μm/s. The size of the micellar assemblies were determined using the option "Particle Analysis" of the Nanoscope software. The values of the radii were not corrected for the finite tip radius. The silicon wafers used as substrates were cleaned with organic solvents (THF, chloroform, and acetone) and subsequently with a stream of CO_2 ice crystals ("snow jet"). The thin films were prepared by dip-coating a silicon wafer in a 0.1 g/L block copolymer solution in THF or by applying a drop of a 1 g/L aqueous solution onto a 100 °C hot silicon wafer, respectively.

For *transmission electron microscopy* (TEM) a CEM 902 electron microscope (Zeiss) was used (acceleration voltage: 80 kV). One 5 μL drop of solution (0.001 mg/L) was applied onto TEM grids covered with a thin silicon film. After drying, the samples were stained with RuO_4 (selective for polystyrene), iodine (selective for amylose), or $CoCl_2$ (accumulates within micelles). The size of the aggregates was evaluated with the graphics software ImageJ 1.16f. For freeze-fracture TEM, drops of polymer solution were shock frozen in liquid ethane and subsequently fractured on a Balzers BAF 400 freeze etching system. Replicas of the freshly exposed fracture surface were prepared following standard procedures.

Results and Discussion

Micellar Aggregates in THF. We start our discussion with the results obtained in THF, which is a good solvent for polystyrene and a nonsolvent for amylose.

Fluorescence Correlation Spectroscopy (FCS). First, the critical micelle concentration (cmc) for the system amylose$_{60}$-*block*-polystyrene$_{740}$ (the subscripts denoting degrees of polymerization) with M_n = 84 000 g/mol was determined by FCS measurements conducted at different polymer concentrations (Figure 1A).[19] For polymer concentrations below 0.1 g/L the autocorrelation function is typical for free fluorescent dye molecules. For concentrations at and above 0.1 g/L, however, the autocorrelation functions can only be fitted satisfactorily by the superposition of a second, larger particle, which we assign to a micelle. From these experiments, which are summarized in Figure 1B, we conclude that micelle formation starts at a cmc in the range between 0.01 and 0.1 g/L. In the same concentrations range, the amplitude of the autocorrelation function decreases significantly. Since $G(\tau)$ scales inversely with the number of dye molecules, N_{dye}, present in the focus, $G(0) \propto 1/N_{dye}+1$, this finding indicates that the total number of dye molecules in the solution increases. This increase can be rationalized as an improved solubilization of dye molecules which before may have been adsorbed on the walls of the FCS cell. All further experiments were conducted at sufficiently high concentrations to ensure that micelles were formed.

Dynamic light scattering (DLS) measurements on block copolymer solutions in THF revealed up to four species of different hydrodynamic radius. Figure 2 shows autocorrelation functions and respective CONTIN plots obtained by DLS measurements at different concentrations. The corresponding hydrodynamic radii are given in Table S-2 (Supporting Information). Large aggregates are already detectable at a concentration (0.0061 g/L) lower than the cmc obtained from FCS. However, it must be taken into consideration that DLS renders a z-distribution (and a z-average) of hydrodynamic radii; i.e., the weight fraction (and even more the

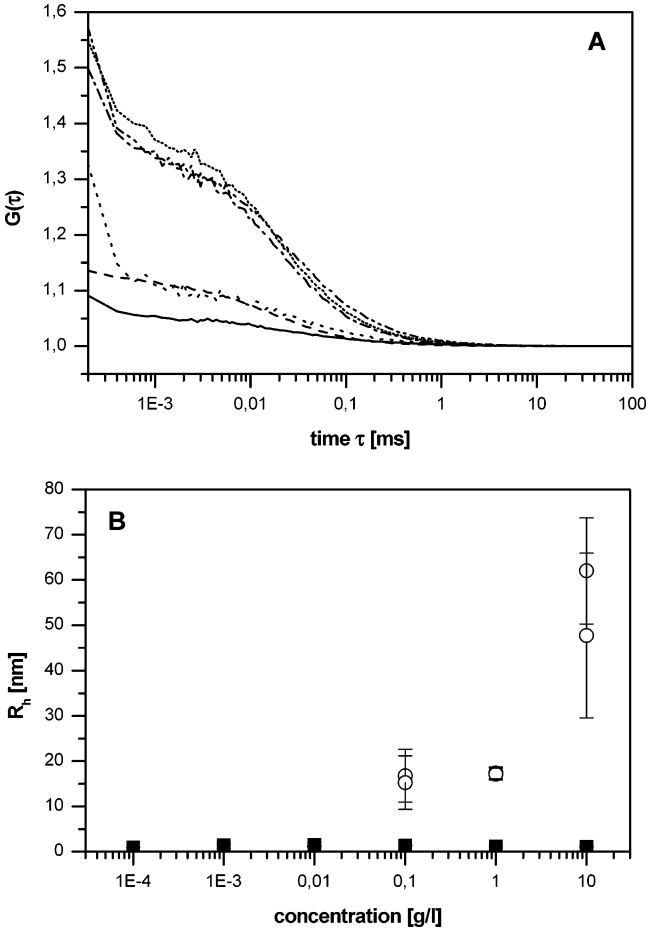

Figure 1. (A) Fluorescence correlation spectroscopy autocorrelation functions of amylose$_{60}$-*block*-polystyrene$_{740}$ in THF at concentrations of (—) 10, (•••) 1, (- - -) 10^{-1}, (-•-) 10^{-2}, (-•••) 10^{-3}, and (• • •) 10^{-4} g/L. (B) Hydrodynamic radii for different concentrations (■, free dye; ○, micelles).

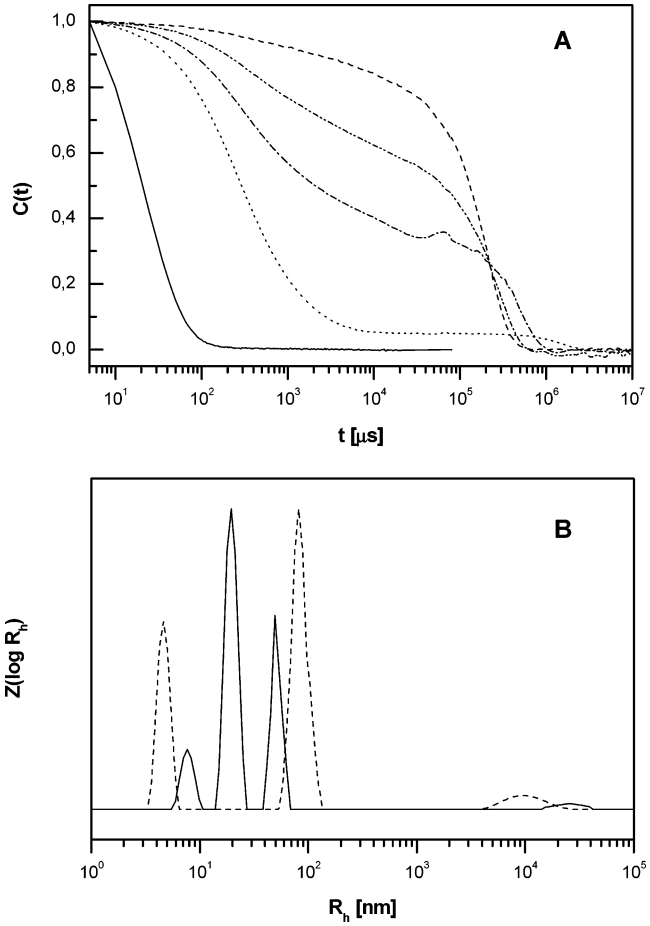

Figure 2. (A) Dynamic light scattering field autocorrelation functions of (—) NH_2-functionalized polystyrene$_{740}$ and amylose$_{60}$-*block*-polystyrene$_{740}$ in THF at different concentrations: (•••) 0.2, (-•-) 0.1, (-•••) 0.067, and (- - -) 0.0061 g/L (angle 30°; temperature 25 °C). (B) Examples for CONTIN plots obtained from autocorrelation functions shown in (A) (—) 0.2 and (- - -) 0.0061 g/L.

number fraction) of the larger species is very low. In contrast, the hydrodynamic radii obtained by FCS are number averages. Consequently, DLS is much more sensitive to the presence of big aggregates which indicates that we are not in the thermal equilibrium. In contrast, the influence of big aggregates on the FCS signal is much smaller. In that point the FCS measurement gives us a cmc value which is closer to the thermal equilibrium than the value obtained by DLS.[20]

Asymmetric flow field flow fractionation (AF-FFF) was used to reassure the different species observed by DLS.[21] The AF-FFF eluogram of amylose$_{60}$-*block*-polystyrene$_{740}$ (Figure 3) clearly shows four distinguishable species separated by the cross-flow. Because of dilution during the separation process, the actual concentration in the flow channel is estimated as 0.1 g/L, i.e., only slightly above cmc. The number-average molecular weight of the first species (peak a, as calculated from the 90° signal of the MALS detector, dn/dc = 0.1481 mL/g) is M_n = 1.06×10^5 g/mol, which is quite close to the molecular weight of block copolymer, indicating that this species is the unimer. The second species (peak b) has a number-average molecular weight of 2.59×10^5 g/mol, which corresponds to small aggregates of block copolymer, presumably dimers and/or trimers. The concentration signals for the other two species (peaks c and d) are so weak (<5% of the total mass) that the accurate analysis of molecular weight of these two species is

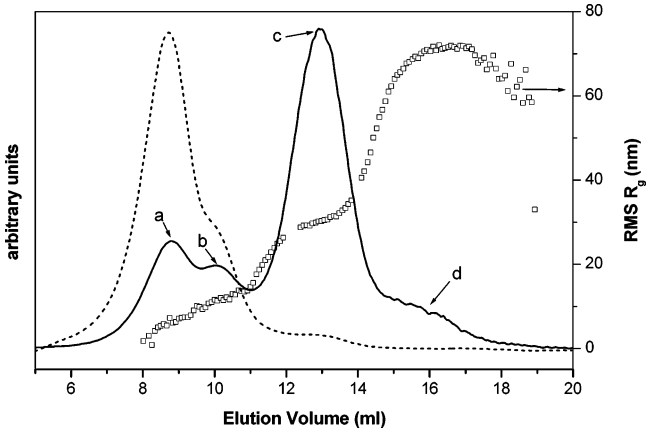

Figure 3. Asymmetric-flow field-flow fractionation measurement of a 6 g/L solution of amylose$_{60}$-*block*-polystyrene$_{740}$ in THF: (- --) UV signal; (—) 90° light scattering signal; (□) radius of gyration distribution obtained using the Debye method. The nominations a to d mark the found four aggregation species.

impossible. However, from the radii of gyration (shown in Figure 3B) one can easily see that these two species are the large aggregates (micelles) with R_g = 30 and 70 nm, respectively. From this result we conclude that the first peak in the CONTIN plots in Figure 2B (R_h < 10 nm) corresponds to either unimers or a mixture of

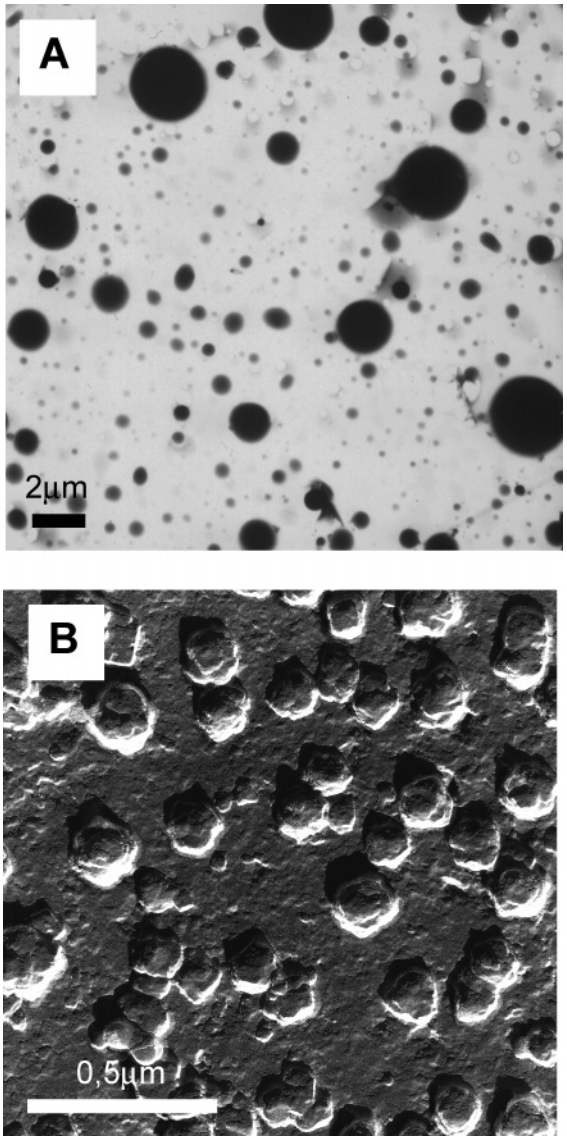

Figure 4. (A) TEM micrographs of polystyrene$_{740}$-*block*-amylose$_{60}$ micellar aggregates from a 1 g/L THF solution. (A) Thin film on a Si-covered TEM grid; $CoCl_2$ stained; scale bar 1 μm. (B) Replica obtained after freeze fracture; scale bar 0.5 μm.

unimers, dimers, and trimers, whereas the second peak ($R_h \approx 20$ nm) is attributed to micelles. The peak at larger radii, although seen in the z-distribution, would be invisible in a weight distribution because the z-fractions have to be divided by the molecular weight which for spherical objects roughly scales as R^3. Thus, the majority of particles appear to be unimers, with a small weight fraction of micelles and a minute weight fraction of very large particles that can be interpreted as vesicle-like structures.

Transmission Electron Microscopy (TEM). The sizes that become obvious from FFF and DLS measurements, especially the "giant" aggregates, are far away from sizes obtainable by normal star micelles. The wide size distribution is visualized in the TEM micrographs in Figure 4 (micelles on a silicon-coated TEM grid and freeze fracture, respectively). On a single TEM grid a large number of different structures were identified, which may in part be due to the fact that by solvent evaporation different concentrations are passed through.

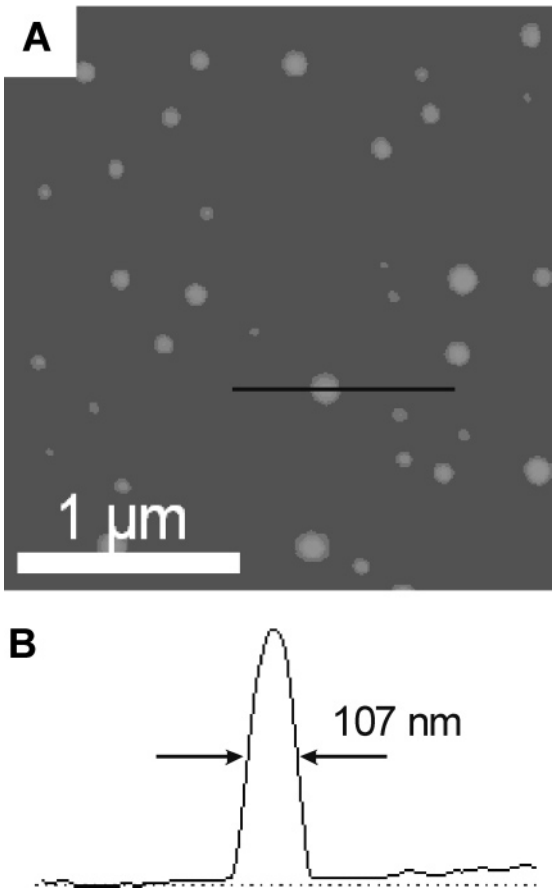

Figure 5. (A) Scanning force microscopic height image of a amylose$_{60}$-*block*-polystyrene$_{740}$ film prepared on a silicon surface from a 0.1 g/L solution in THF (z range 100 nm). (B) Cross section taken from image (A).

Scanning Force Microscopy (SFM). It is also possible to visualize the block copolymers after dip-coating from THF solution by SFM (Figure 5). After drying, we find isolated pancake-shaped objects on the surface. From the SFM height images, we can determine the radii of the collapsed micelles (Figure 5 B and Table S-3 (Supporting Information)).

Scaling laws for the star micelles in THF were estimated from the hydrodynamic radii of the smallest micelles and from the number-average SFM radii. Since they relate to nonequilibrium structures only, they are given in the Supporting Information (Table S-4, Figure S-1)

Micellar Aggregates in Water. Since amylose is water-soluble and $N_{amylose} < N_{polystyrene}$ for all polymers investigated we expect the formation of crew-cut micelles in water. To obtain aqueous solutions of amylose-*block*-polystyrene, a single solvent approach was used: The system was heated to 200 °C at a pressure of 15 bar overnight. The alternative approach with a common solvent for both blocks and subsequent exchange with a nonsolvent for the longer block was not possible in our system because there are no common solvents for amylose and polystyrene.

Micelles were detectable by DLS (see Table 1) and visualized by SFM and TEM. As can be seen in Figure 6, the resulting aggregates are much more uniform in size than the micelles of the same composition in THF. In the TEM micrographs we find a large fraction of objects with round shape and typical diameters of 10−

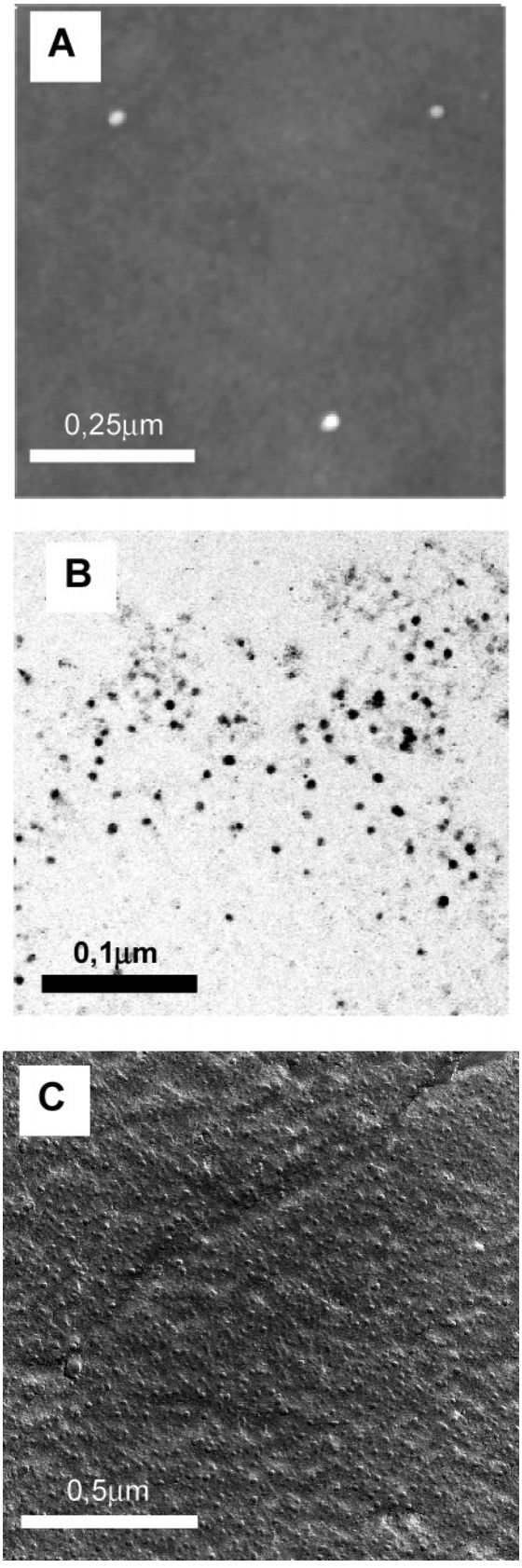

Figure 6. Microscopic images of crew-cut micelles (polystyrene$_{740}$-*block*-amylose$_{60}$ from water: (A) SFM (height, z range 20 nm); (B) TEM (iodine-stained film on a Si-covered grid); (C) TEM after freeze fracture.

30 nm, depending on the composition, which we attribute to crew-cut micelles. In addition, a very small fraction of smaller objects is found (diameters between 4 and 10 nm, depending on composition), which may be identified as single molecules or very small aggregates.

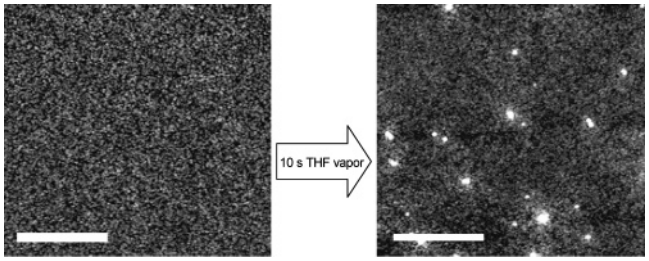

Figure 7. SFM height images of crew-cut micelles from amylose$_{60}$-*block*-polystyrene$_{740}$ in water before and after treatment with THF vapor (scale bar 1 μm; z range 15 nm).

The obtained crew-cut micelles are stable in solution and in bulk. Freeze-dried samples of the micelles dissolve very slowly (over days) in THF. Figure 7 shows an SFM height image of a closed film of crew-cut aggregates. After exposing this film to THF vapor, only a few aggregates swell. This behavior was found over the entire film area and by repeated treatment with THF vapor more crew-cut aggregates swell over the entire film.

We performed DLS and SFM experiments for a variety of different block copolymer compositions at a copolymer concentration of 1 g/L in water. From bilogarithmic plots (Figure 8) scaling laws were determined for the dependence of the micellar size (z-average for R_h and number-average for SFM) on the respective chain length of the blocks. The collapsed aggregates on silicon surfaces obey approximately the relations $R \propto N_{core}^{1/4}$ and $R \propto N_{corona}^{1/2}$.

The crew-cut micelles in aqueous solution approximately scale with $R \propto N_{core}^{1/4}$ and $R \propto N_{corona}^{1/6}$. This illustrates that the insoluble block (polystyrene) has a larger influence on the micellar size than the soluble block (amylose). This is reasonable as the polystyrene block is by far the longer block and therefore has the larger influence on the aggregate size. In addition, the amylose block is not swollen in water, and because it is a helical molecule, the elongation of the amylose block does not result in a large increase of the corona dimension.

Conclusion

Amylose-*block*-polystyrene block copolymers form aggregates of different sizes in THF and crew-cut micelles of rather uniform size in water.

The large number of aggregates with different sizes indicates that these structures are not in a thermal equilibrium, but rather frozen in the process of the preparation of the solution. In contrast, the crew-cut micelles prepared at 200 °C in water are assumed to have been in equilibrium above the glass transition temperature of polystyrene ($T_g \cong 105$ °C). Thus, the observed structures may represent equilibrium structures which were frozen upon cooling below T_g. The structures of these micelles differ from classical ones by the rodlike, helical structure of the corona which is not taken into account by current theories.

Presently, neither the exact nature of the aggregates nor their aggregation numbers are accessible by our experiments. Further experimental work is needed to establish a more complete picture.

The block length dependence of the aggregate sizes is in agreement with earlier predictions as well as

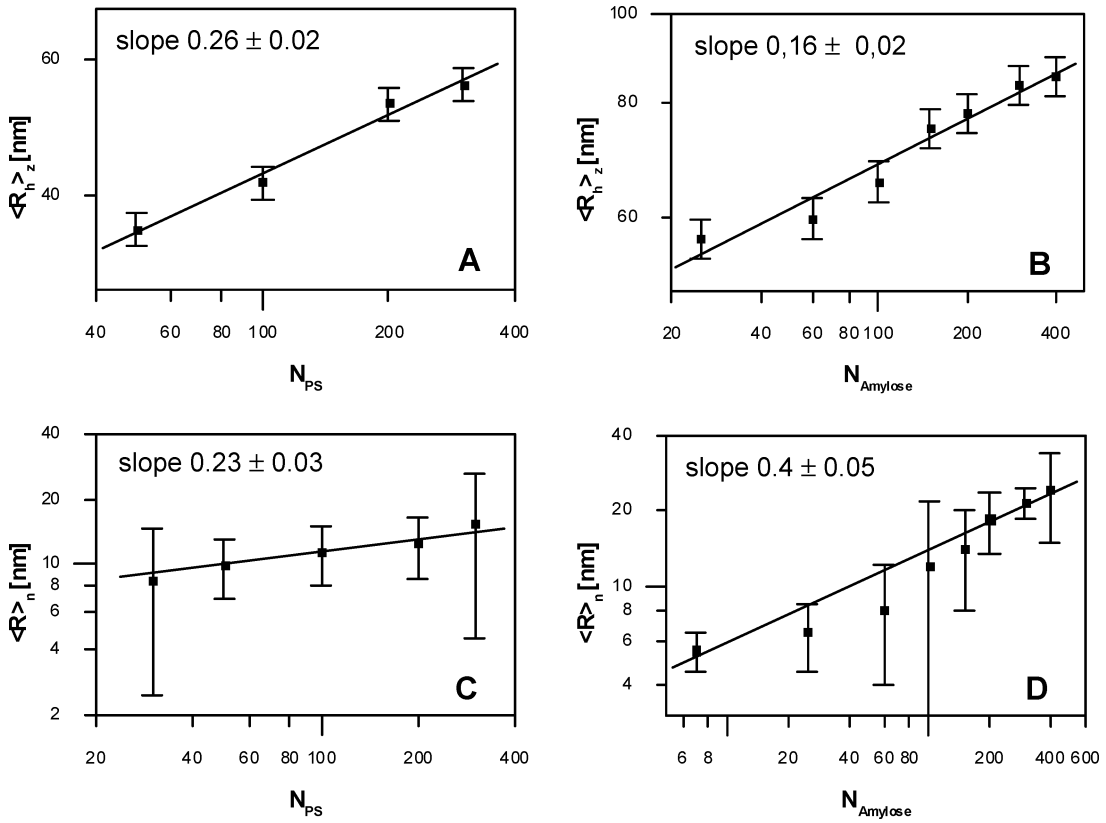

Figure 8. Dependence of the observed radii on the block lengths in water, as determined by DLS, (A) + (B), and SFM, (C) + (D).

experiments, but we note that different theoretical approaches have predicted different scaling exponents varying from $0.5 \leq z \leq 1$ (in $R \propto N^z$).[22] Experimental values found for block copolymer systems also show a large variation.[22]

Theories on the aggregation number and size of crew-cut micelles in solution vary, depending on the type of block copolymer and the quality of the solvent used. Whitmore and Noolandi studied polystyrene-*b*-polybutadiene micelles dissolved in polybutadiene using free energy minimization and found a weak influence of the soluble block as well.[23a] This is in contrast to the theories of Nagarajan and Ganash[23b] and of Zhulina and Birshtein,[23c] who predict a larger influence of the soluble block for polystyrene-*b*-polybutadiene, poly(ethylene oxide)-*b*-poly(propylene oxide), and polystyrene-*b*-poly(acrylic acid) crew cut micelles in good solvents for the outer block. Eisenberg et al. also found a considerable influence of the soluble block for polystyrene-*b*-poly(acrylic acid) crew-cut micelles in water by TEM and DLS studies.[23d]

There are not as many theoretical considerations for crew-cut as for star-type micelles which makes a comparison of our results with theories not easy. Further, our system is complicated by the conformational asymmetry between the two blocks, the helicicity of the amylose block, and the strong tendency of the amylose to crystallize which prevents any reasonable comparison with current theories.

In addition, the block copolymer system discussed here are more complex than the systems found in the literature by the conformational asymmetry between the two blocks, the helicicity of the amylose block, and the strong tendency of the amylose to crystallize.

Because of the big variation of theoretical consideration and experimental results, it will be necessary to establish a larger number of experimental results with different block copolymer systems in the future, and this paper is part of this effort.

Acknowledgment. The authors are indebted to Dimitrios Samios, Clèia de Andrade Salles (Universidade Federal do Rio Grande do Sul, Brazil), and Werner Köhler (Universität Bayreuth, Germany) for their help with the light scattering experiments. We also thank Astrid Göpfert for the TEM micrographs and Klaus Horbatschek for the freeze-fracture experiments. Helpful discussions with Oleg Borisov are greatly acknowledged.

Supporting Information Available: Tables S-1 to S-4 and Figure 4. This material is available free of charge via the Internet at http://pubs.acs.org.

References and Notes

(1) (a) Bates, F.; Fredrickson, G. H. *Annu. Rev. Phys. Chem.* **1990**, *41*, 525. (b) Hamley, I. W. *Block Copolymers*; Oxford University Press: Oxford, 1999.
(2) (a) Leibler, L. *Macromolecules* **1980**, *13*, 1602. (b) Matsen, M. W.; Bates, F. S. *J. Chem. Phys.* **1997**, *106*, 2436.
(3) (a) Raphael, E.; de Gennes, P. G. *Makromol. Chem., Macromol. Symp.* **1992**, *62*, 1. (b) Semenov, A. N.; Subbotin, A. V. *Sov. Phys. JETP* **1992**, *74*, 660. (c) Matsen, M. W.; Barrett, C. *J. Chem. Phys.* **1998**, *109*, 4108. (d) Halperin, A. *Europhys. Lett.* **1989**, *10*, 549. (e) Halperin, A. *Macromolecules* **1990**, *23*, 2724. (f) Sevick, E. M.; Williams, D. R. M. *Colloids Surf.* **1997**, *129−130*, 387.
(4) (a) Perly, B.; Douy, A.; Gallot, B. *Makromol. Chem.* **1976**, *177*, 2569. (b) Nakajima, A.; Hayashi, T.; Kugo, K.; Shinoda, K. *Macromolecules* **1979**, *12*, 840. (c) Barenberg, S.; Anderson, J. M.; Geil, P. H. *Int. J. Biol. Macromol* **1981**, *3*, 82. (d) Klok, H.-A.; Langenwalter, J. F.; Lecommandoux, S. *Macromolecules* **2000**, *33*, 7819. (e) Kukula, H.; Schlaad, H, Antonietti, M.; Förster, S. *J. Am. Chem. Soc.* **2002**, *124*, 1658.
(5) Rowan, A. E.; Nunen, J. L. M.; Schenning, A. P. H. J.; Nolte, R. J. M. *Macromol. Symp.* **1996**, *102*, 217.
(6) Chen, J. T.; Thomas, E. L.; Ober, C. K.; Mao, G.-P. *Science* **1996**, *273*.

(7) David, J. L.; Gido, S. P.; Novak, B. M. *Polym. Prepr.* **1984**, 433.
(8) Krigbaum, W. R.; Preston, J.; Ciferri, A.; Shufan, Z. *J. Polym. Sci.* **1987**, *25*, 653.
(9) Francois, B.; Zhong, X. F. *Synth. Met.* **1991**, *41*, 955.
(10) (a) Jenekhe, S. A.; Chen, X. L. *Science* **1998**, *279*, 1903. (b) Jenekhe, S. A.; Chen, X. L. *Science* **1999**, *283*, 372.
(11) (a) Stupp, S. I.; Keser, M.; Tew, G. N. *Polymer* **1998**, *39*, 4505. (b) Lee, M.; Cho, B.-K.; Kang, Y.-S.; Zin, W.-C. *Macromolecules* **1999**, *32*, 8531. (c) Lee, M.; Cho, B.-K.; Zin, W.-C. *Chem. Rev.* **2001**, *101,* 3869.
(12) (a) Bates, F. S.; Schulz, M. F.; Rosedale, J. H.; Almdal, K. *Macromolecules* **1992**, *25*, 5547. (b) Singh, C.; Goulian, M.; Liu, A. J.; Fredrickson, G. H. *Macromolecules* **1994**, *27*, 2974.
(13) Loos, K.; Munoz-Guerra, S. In *Supramolecular Polymers*; Ciferri, A., Ed.; Marcel Dekker: New York, 2000.
(14) Halperin, A.; Tirrell, M.; Lodge, T. P. *Adv. Polym. Sci.* **1992**, *100*, 31.
(15) (a) Shen, H. W.; Zhang, L. F.; Eisenberg, A. *J. Phys. Chem. B* **1997**, *101*, 4697. (b) Yu, K.; Zhang, L. F.; Eisenberg, A. *Langmuir* **1996**, *12*, 5980. (c) Yu, K.; Eisenberg, A. *Macromolecules* **1996**, *29*, 6359. (d) Yu, Y. S.; Eisenberg, A. *J. Am. Chem. Soc.* **1997**, *119*, 8383. (e) Yu, Y.; Zhang, L.; Eisenberg, A. *Macromolecules* **1998**, *31*, 1144. (f) Zhang, L. F.; Eisenberg, A. *Science* **1995**, *268*, 1728. (g) Massey, J.; Power, K. N.; Manners, I.; Winnik, M. A. *J. Am. Chem. Soc.* **1998**, *120*, 9533. (h) Henselwood, F.; Liu, G. *Macromolecules* **1998**, *31*, 4213. (i) Gao, Z. S.; Varshney, S. K.; Wong, S.; Eisenberg, A. *Macromolecules* **1994**, *27*, 7923.
(16) Gündüz, S.; Dincer, S. *Polymer* **1980**, *21*, 1041.
(17) Desbaumes, L.; Eisenberg, A. *Langmuir* **1999**, *15*, 36.
(18) (a) Loos, K.; Müller, A. *Biomacromolecules* **2002,** *3*, 368. (b) Loos, K.; Stadler, R. *Macromolecules* **1997**, *30*, 7641.
(19) (a) Erhard, R.; Böker, A.; Zettl, H.; Kaya, H.; Pyckhout-Hintzen, W.; Krausch, G.; Abetz, V.; Müller, A. H. E. *Macromolecules* **2001**, *34*, 1069. (b) Schuch, H.; Klingler, J.; Rossmanith, P.; Frechen, T.; Gerst, M.; Feldthusen, J.; Müller, A. H. E. *Macromolecules* **2000**, *33*, 1734.
(20) Matejicek, P.; Humpolickova, J.; Prochazka, K.; Tuzar, Z.; Spirkova, M.; Hof, M.; Webber, S. E. *J. Phys. Chem. B* **2003**, *107*, 8232.
(21) (a) Cölfen, H.; Antonietti, M. *Adv. Polym. Sci.* **2000**, *150*, 67. (b) Martin, M. *Adv. Chromatogr.* **1998**, *39*, 1. (c) Myers, M. N. *J. Microcolumn Sep.* **1997**, *9*, 151.
(22) Förster, S.; Zisenis, M.; Wenz, E.; Antonietti, M. *J. Chem. Phys.* **1996**, *104*, 9956.
(23) (a) Whitmore, M.; Noolandi, J. *Macromolecules* **1985**, *18*, 657. (b) Nagarajan, R.; Ganesh, K. *J. Chem. Phys.* **1989**, *90*, 5843. (c) Zhulina, E. B.; Birshtein, T. M. *Vysokomol. Soedin.* **1985**, *27*, 511. (d) Zhang, L.; Raymond, J. B.; Eisenberg, A. *Macromolecules* **1995**, *28*, 6055.

MA0345549